

ISTITUTO NAZIONALE DI FISICA NUCLEARE

Sezione di Milano

INFN/TC-88/8

17 Febbraio 1988

R. Bonifacio, B.W.J. Mc Neil, P. Pierini:

SLIPPAGE AND SUPERRADIANCE IN THE HIGH-GAIN FEL

Slippage And Superradiance In The High-Gain FEL

*R. Bonifacio, B.W.J.McNeil *, P. Pierini*

Dipartimento di Fisica, Università di Milano — INFN Sezione di Milano

ABSTRACT

In this paper we describe the Single-Pass High-Gain Free Electron Laser Amplifier taking into account propagation effects, (*i.e.* Slippage).

We demonstrate the existence of two different dynamical regions characterized by an adimensional parameter K such that K^{-1} is a measure of the gain of a photon on slipping through the electron pulse.

We define the long pulse limit to be when $K \ll 1$. In this case we find that only the leading region of the propagating radiation pulse exhibits the previous steady-state behaviour with peak power proportional to $n_e^{4/3}$ (where n_e is the electron beam density). The trailing (slippage) region exhibits a spiking behaviour with peak intensities reaching ten times the saturated intensity predicted by steady-state theory.

The existence of the spiking may be related to the fact that the trailing region of the electron pulse experiences less radiation re-absorption than the leading region, so that slippage inhibits saturation.

The energy extracted from the beam exhibits the well known oscillatory behaviour after saturation as predicted by the steady-state theory.

We define the short-pulse regime to be when $K > 1$. In this regime the peak power emitted by the electrons does not scale as $n_e^{4/3}$, as predicted by steady-state theory, but scales as n_e^2 , which is typical of superradiant behaviour.

Furthermore, energy is extracted from the electrons in a continuous way, with no steady-state type oscillatory behaviour, so that the efficiency of the superradiant FEL may be enhanced considerably.

1. – INTRODUCTION

In this paper we investigate pulse propagation effects in a Single-Pass High-Gain FEL amplifier^(1a,1b).

* *Supported by The Royal Society under the European Science Exchange Programme*

The radiation evolution from both long and short electron pulses are investigated enabling further examination of the predicted Superradiant Regime of the single-pass FEL⁽²⁾.

Pulse propagation simulation is carried out by a computer code which models the electron and radiation pulses by a 1-D distribution of radiation and electron beam parameters. This enable the slippage of the radiation through the electron pulse to be modeled effectively for a wide range of electron pulse widths.

Most previous theories for the single-pass amplifier assume an infinitely long, uniform density electron beam, so that one section of the electron beam (and hence radiation) evolves identically with all other sections as it passes through the wiggler⁽³⁾ and References therein).

In simulations which have included pulse effects (*e.g.* ⁽⁴⁾) the electron pulses were assumed long and the evolution of the electrons and radiation in the leading and trailing regions of the pulses were ignored by using the "wrapped-window approximation".

In the long pulse simulation here we make no such approximations and allow the electron and radiation pulses evolve over their entire lengths. This allows new effects in the trailing region of the radiation pulses to be investigated.

In chapter 2 we give a brief account of the equations and computational methods used.

In chapter 3 we use the model to investigate Long Pulse propagation; Short Pulse and Superradiance are considered in chapter 4.

Chapter 5 gives a discussion and summary of the results obtained.

2. - COMPUTATIONAL MODEL

The equations used to describe the 1-D pulse evolution of the radiation and electrons are the partial differential form of the coupled Maxwell-Pendulum equations⁽⁵⁾

$$\left(\frac{\partial}{\partial z} + \frac{1}{c} \frac{\partial}{\partial t} \right) a(z, t) = j(z, t) \langle e^{-i\theta(z, t)} \rangle \quad (1)$$

$$\left(\frac{\partial}{\partial z} + \frac{1}{c\beta_{\parallel}} \frac{\partial}{\partial t} \right)^2 \theta_m(z, t) = \left(a(z, t) e^{i\theta_m(z, t)} + c.c. \right) \quad m = 1, \dots, N \quad (2)$$

where familiar notation has been used.

By transforming to the characteristics

$$\begin{cases} z_1 = z - c\beta_{\parallel}t \\ z_2 = ct - z \end{cases} \quad (3)$$

we obtain

$$(1 - \beta_{\parallel}) \frac{\partial}{\partial z_1} a(z_1, z_2) = j(z_1) \langle e^{-i\theta(z_1, z_2)} \rangle \quad (4)$$

$$\frac{(1 - \beta_{\parallel})^2}{\beta_{\parallel}^2} \frac{\partial^2}{\partial z_2^2} \theta_m(z_1, z_2) = - \left(a(z_1, z_2) e^{i\theta_m(z_1, z_2)} + c.c. \right) \quad m = 1, \dots, N \quad (5)$$

Similarly to Ref.^(1a) we transform to dimensionless variables. We define

$$\begin{cases} \bar{z}_1 = \frac{4\pi\rho}{\lambda_R\beta_{\parallel}}z_1 \\ \quad = \frac{4\pi\rho}{\lambda_R\beta_{\parallel}}(z - c\beta_{\parallel}t) \\ \bar{z}_2 = \frac{4\pi\rho}{\lambda_R}z_2 \\ \quad = \frac{4\pi\rho}{\lambda_R}(ct - z) \end{cases} \quad (6)$$

where

$$\rho = \frac{1}{\langle \gamma_R \rangle} \left(\frac{a_0 \omega_P \lambda_0}{4 \cdot 2\pi c} \right)^{2/3} \quad (7)$$

is the fundamental FEL parameter^(1a), which scales as $n_e^{1/3}$, and: $\langle \gamma_R \rangle$ is the resonant electron energy (in units of mc^2), λ_0 is the wiggler period, ω_P is the non-relativistic plasma frequency defined as $\left(\frac{4\pi e^2 n_e}{m} \right)^{1/2}$, $a_0 = \frac{eB_w \lambda_0}{2\pi mc^2}$ is the undulator parameter, n_e is the electron density.

We assume resonance, *i.e.* the radiation wavelength is given by:

$$\lambda_R = \lambda_0 \frac{1 - \beta_{\parallel}}{\beta_{\parallel}} \simeq \frac{\lambda_0}{2\gamma_R^2} (1 + a_0^2) \quad (8)$$

which implies that one wavelength of radiation passes over a resonant electron in one wiggler period. In this way equations (4)–(5) become

$$\frac{\partial}{\partial \bar{z}_1} A(\bar{z}_1, \bar{z}_2) = f(\bar{z}_1) \langle e^{-i\theta(\bar{z}_1, \bar{z}_2)} \rangle \quad (9)$$

$$\frac{\partial^2}{\partial \bar{z}_2^2} \theta_m(\bar{z}_1, \bar{z}_2) = - \left(A(\bar{z}_1, \bar{z}_2) e^{i\theta_m(\bar{z}_1, \bar{z}_2)} + c.c. \right) \quad m = 1, \dots, N \quad (10)$$

Here $f(\bar{z}_1)$ is the macroscopic electron density function normalized to one and A is the dimensionless field amplitude^(1a) defined so that

$$|A|^2 = \frac{|E_0|^2 / 4\pi}{n_e \langle \gamma_R \rangle mc^2 \rho} \quad (11)$$

where E_0 is the electric field amplitude.

Note that \bar{z}_1 and \bar{z}_2 are normalized to the “cooperation length” of Ref.^(1a)

$$L_c = \frac{\lambda_R}{4\pi\rho} \quad (12)$$

The two coordinates \bar{z}_1 and \bar{z}_2 slip by $4\pi\rho$ when $\Delta z = \lambda_0$, if the resonance condition (8) is satisfied:

$$\Delta(\bar{z}_1 + \bar{z}_2) = \frac{4\pi\rho}{\lambda_R} \left(\frac{1}{\beta_{\parallel}} - 1 \right) \Delta z = \frac{4\pi\rho}{\lambda_0} \Delta z = 4\pi\rho$$

Furthermore \bar{z}_1 and \bar{z}_2 change in steps of $4\pi\rho$ per wiggler period along the characteristics $\bar{z}_2 = \text{const.}$ and $\bar{z}_1 = \text{const.}$, respectively:

$$\begin{aligned} \Delta \bar{z}_1 = 4\pi\rho \quad \text{for} \quad \Delta z = \lambda_0 \quad \text{and} \quad \bar{z}_2 = \text{const.} \quad \text{i.e.} \quad \Delta z = c\Delta t \\ \Delta \bar{z}_2 = 4\pi\rho \quad \text{for} \quad \Delta z = \lambda_0 \quad \text{and} \quad \bar{z}_1 = \text{const.} \quad \text{i.e.} \quad \Delta z = c\beta_{\parallel}\Delta t \end{aligned}$$

Note from (6) that $\Delta\bar{z}_1 = \Delta\bar{z}_2 = 4\pi\rho$ corresponds to $\Delta z \simeq \lambda_R$ (for t constant), i.e. $\frac{\lambda_R}{L_c} = 4\pi\rho$.

Hence the "natural" unit length in which to discretize both the electron pulse and the radiation pulse is $4\pi\rho$ (i.e. λ_R). The equations are then integrated with step size $\Delta\bar{z}_1 = \Delta\bar{z}_2 = 4\pi\rho = \Delta\tau$ repeated through N_o wiggler periods so that the total integration interval is $4\pi\rho N_o$, i.e. the total unsaturated gain^(1a). Furthermore after each integration step we let the electron pulse slip behind the radiation pulse by one wavelength λ_R ($4\pi\rho$), so that at the end the total slippage will be $N_o\lambda_R$ as required by the resonance condition (8).

It is useful to summarize the parameters associated with pulse propagation effects, in the system of dimensionless units of Ref's.^(1a,2):

- $G = 4\pi\rho N_o$ is the total unsaturated gain ($G \gg 1$) in the steady state limit,
- L_b is the electron pulse length,
- $S = \frac{N_o\lambda_R}{L_b} = \frac{N_o}{N_b}$ is the slippage parameter ($N_b \equiv \frac{L_b}{\lambda_R}$)
and in accord with Ref.⁽²⁾ we define the *Superradiant Parameter* K as:

$$K \equiv \frac{L_c}{L_b} = \frac{S}{G} = \frac{1}{4\pi\rho N_b} \quad (13)$$

Note that K^{-1} is a measure of the gain of a photon on slipping through the electron pulse. Also K is equal to the slippage, S , when $N_o = \frac{1}{4\pi\rho}$, or $G = 1$.

3. - THE LONG PULSE LIMIT: $K \ll 1$, ($L_b \gg L_c$)

In this section we use the computational model, described in the previous section, to re-examine the output from the Single-Pass Amplifier in the Long electron Pulse (L.P.) Limit.

Unlike previous theories where this regime was characterized by the slippage parameter $S \ll 1$, we will show that this regime is more correctly characterized by the more stringent condition:

$$K \ll 1 \quad \Rightarrow \quad L_b \gg L_c \quad (14)$$

From previous theories for infinitely long electron pulses ($S = 0$) the dimensionless intensity $|A|^2$ rises exponentially from a noise source term to a saturated value $|A|_{sat}^2 \simeq 1.4$ (Ref.⁽²⁾). It then oscillates at a frequency determined by the synchrotron or sideband oscillation.

For the purpose of investigating long pulse effects here we inject an electron pulse (say) 200 radiation wavelengths long. (This corresponds to 200 electron-pulse "strips" in the computational simulation, one strip corresponding to a discretized element of width λ_R). We have assumed a square electron density distribution so that the function $f(\bar{z}_1) = 1$ throughout the electron pulse. The wiggler has 100 periods, so that the slippage parameter is $S = 0.5$ and $K = 1/60$.

In table 1 we resume the parameters used for this run.

Table 1.

"Long Bunch" parameters						
N_o	N_b	ρ	$\Delta\tau = 4\pi\rho$	G	S	K
100	200	0.02	1/3	30	0.5	1/60

Computational output of the electron and radiation pulse takes the following format: the radiation intensity $|A|^2$ is plotted in a "window" travelling at velocity c at various positions through the wiggler.

The width of the window (in units of radiation wavelengths) is given by the width of the electron pulse plus the distance by which the electron pulse slips with respect to the radiation in the wiggler, *i.e.* $N_b + N_o$.

The electron pulse parameter $\langle \dot{\theta} \rangle$ — corresponding to the “energy loss per strip” — is plotted in a similar type window of width N_b above the radiation pulse. Since the electrons travel at velocity $\beta_{||}c < c$, the electron pulse window is seen to slip behind the radiation pulse window. This slippage is determined by the resonance condition and is then equal to “one strip per wiggler period”. In this way both electron and radiation pulse parameters (here $\langle \dot{\theta} \rangle$ and $|A|^2$) may be plotted at various points through the wiggler.

In Fig.1 we show this series of plots as the radiation–electron pulses pass through the wiggler.

The windows of the electron–radiation pulses have their leading edge synchronous at the start of the wiggler, not shown in the figure. The radiation window is “seeded” with a small uniform field — $|A|^2 = 2 \times 10^{-4} \ll |A|_{sat}^2$ — and the electrons are uniformly distributed in pendulum phase θ with detuning parameter $\dot{\theta} = 0$.

Evolution in the leading regions of the electron–radiation pulses follow a steady–state behaviour, indeed the steady–state evolution of the radiation can be followed as it escapes the leading edge of the electron pulse.

At the trailing edge of the electron pulse there is a region in which the parameters of each electron strip do not evolve identically. This is because there are no electrons behind them and so there is less radiation propagating into this region. The electrons are then radiating practically in the vacuum, *i.e.* spontaneously. This trailing edge of the electrons can then be considered to be intrinsically a large slippage region.

The width of this region in the electron pulse after N_P wiggler periods is N_P radiation wavelengths (strips) from the trailing edge.

This region of pulse evolution has not been investigated before (to the authors’ knowledge).

It is seen that radiation emitted from this portion of the electron pulse is quite different in nature from the steady–state one. Large spikes of high peak intensity are seen to evolve, with peaks reaching a factor of 10 greater than the steady–state intensity of $|A|_{sat}^2 \simeq 1.4$.

The pulse evolution in this region is clearly a result of the slippage of the trailing edge of the electron pulse.

A further consideration for the explanation of these phenomena is the sideband instability: electrons entering the region of high slippage after saturation of the leading edge of the pulse will be executing synchrotron oscillations possibly contributing energy to the spike in a resonant way. The behaviour of this region and particularly of the spikes may then be considered, speculatively, as a “Superradiant Sideband Instability”.

Clearly further work, perhaps in the form of Fourier analysis of the radiation pulse, is required.

A parameter which measures the ability of the system to extract energy from the electron beam may be defined as:

$$E_L = \frac{\text{Total energy of radiation pulse (units } |A|^2)}{N_b} \quad (15)$$

This parameter E_L then gives the average energy extracted from the electron pulse in units of $|A|^2$.

As seen in Fig.2, which plots E_L as a function of the position down the wiggler, E_L oscillates after saturation in a similar way as would be expected from the steady–state theory with maximum $E_L \simeq 1.4$

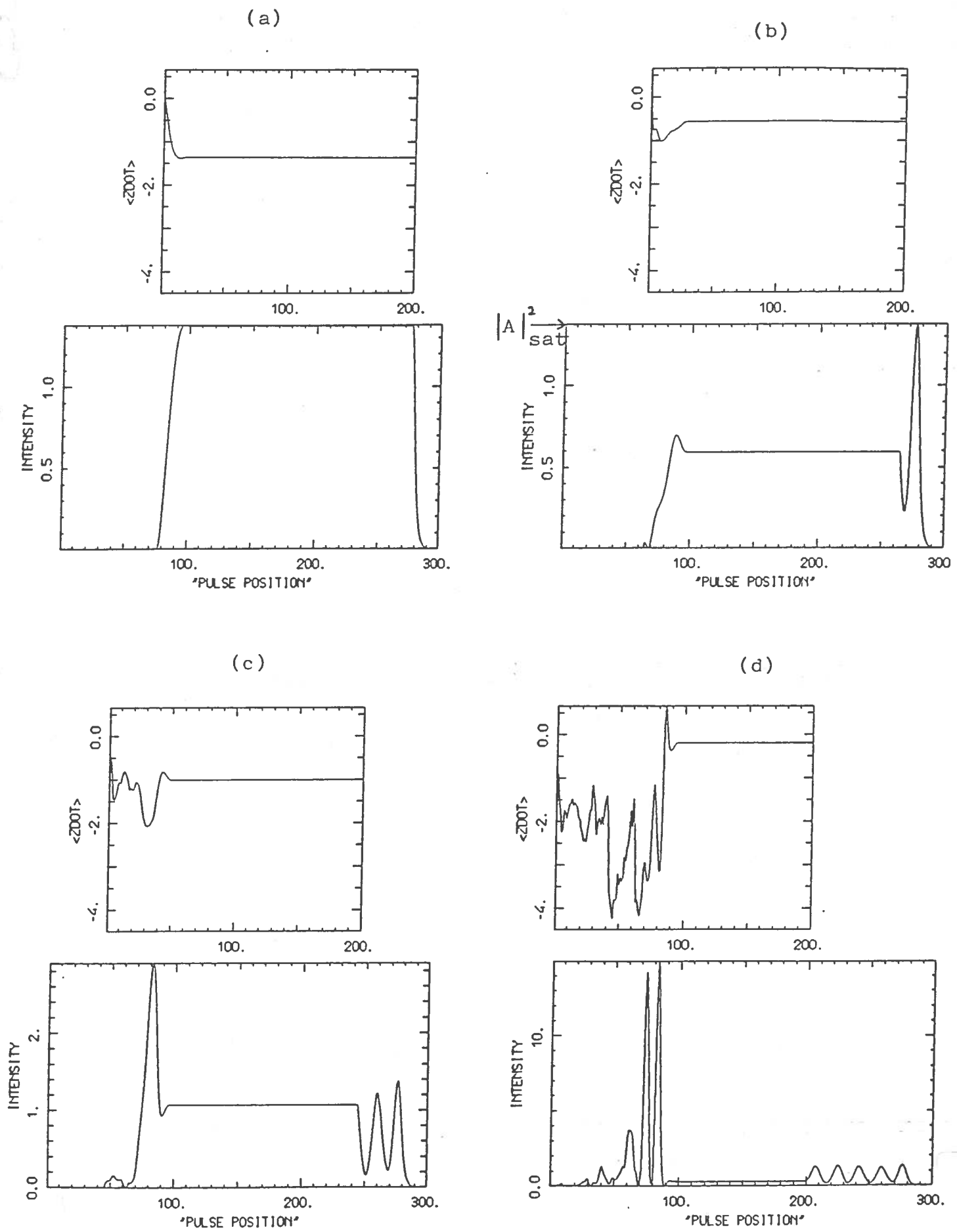


Fig.1. Radiation and electron pulses after N_P wiggler periods are shown in a) to d) for $N_P = 24, 36, 56, 100$ respectively. $N_o = 100$, $N_b = 200$ and $G = 30.0$. A "Top hat" electron density function was used — $f(\bar{z}_1) = 1$ over the electron pulse.

— the spike behaviour has little effect in the actual energy extracted from the electron pulse — so that in this sense the steady-state and pulsed models agree.

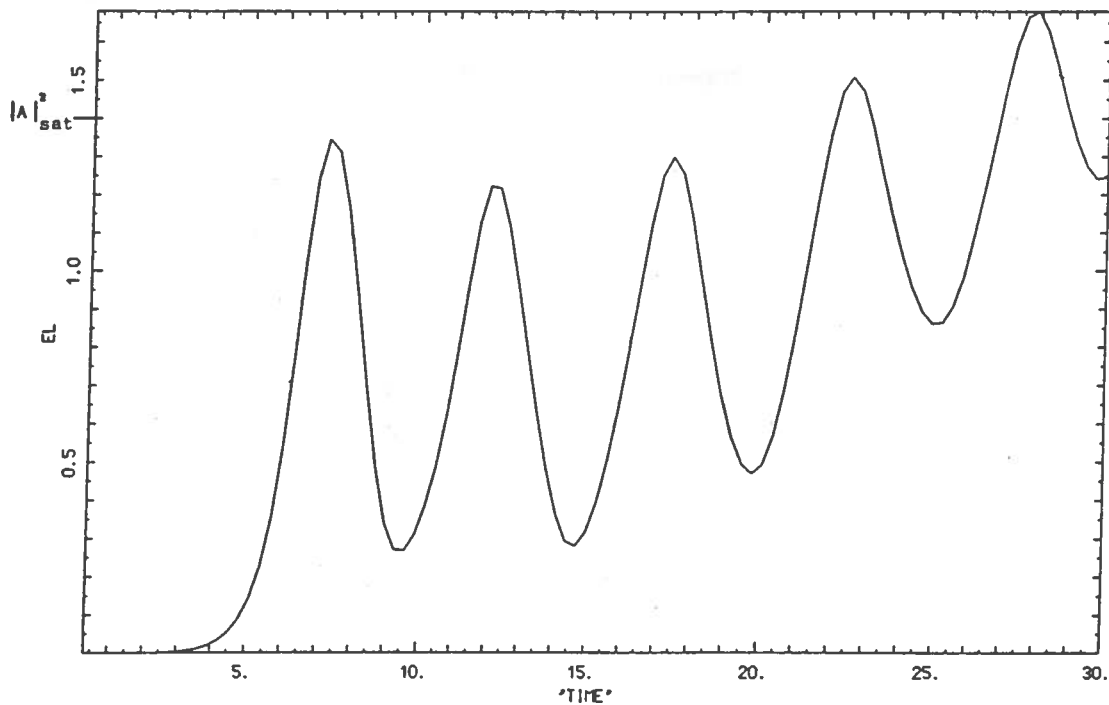


Fig. 2 E_L as a function of dimensionless time, $\tau = 4\pi\rho$, through the wiggler

4. - SHORT PULSE LIMIT: $K > 1$, ($L_h < L_c$)

We now use the computational model to investigate the High-Gain Single-Pass FEL with short electron pulses. In particular we wish to investigate the Superradiant (S.R.) regime first predicted in Ref.(2).

It was suggested that radiation emitted by a sufficiently short electron pulse could quickly "escape" from it — due to the slippage — thereby reducing saturation effects within the pulse.

The escape of emitted radiation has been modeled in the steady-state equations by an exponential loss term of the radiation field.

$$\text{Radiation loss} \propto e^{-K\bar{z}}$$

where \bar{z} is the dimensionless distance traveled through the wiggler and K is the superradiant parameter as defined in chapter 2. Superradiance was determined to occur when $K \gg 1$ and $S > 1$.

With these values it can be shown that the emitted intensity of radiation becomes proportional to n_e^2 instead of the $n_e^{4/3}$ dependence in the steady-state regime. From (7) and (11)

$$|A|^2 \propto \frac{|E|_o^2}{\rho n_e} \quad \text{and} \quad \rho \propto n_e^{1/3}$$

hence the $|A|^2$ scaling goes as:

$$\begin{array}{ll} |A|^2 \propto \rho^0 & \text{for the steady-state} \quad (|E|_o^2 \propto n_e^{4/3}) \\ \text{and} & \\ |A|^2 \propto \rho^2 & \text{for Superradiance} \quad (|E|_o^2 \propto n_e^2) \end{array}$$

Another interpretation of the superradiance parameter K is that as $G = 4\pi\rho N_o$ (steady-state) then K^{-1} is the gain experienced by a photon on traversing the electron pulse (one interaction length, *i.e.* $L_i = \frac{L_b\beta_{\parallel}}{1-\beta_{\parallel}}$). This gives an alternative definition of S as “the number of interaction lengths in the complete wiggler”.

These definitions aid a clearer understanding of the S.R. process as will be shown later.

The same procedure for the representation of both radiation and electron pulses is used as in the previous chapter.

The parameters considered for the series of radiation–electron pulses shown in Fig.3 are:

Table 2.

“Short Bunch” parameters						
N_o	N_b	ρ	$\Delta\tau = 4\pi\rho$	G	S	K
60	6	0.026	1/3	20	10	1/2

We see here that the electron pulse is now much shorter than the previous L.P. limit and so the effect of slippage is much more dramatic: the radiation is escaping more rapidly and so is no longer interacting with the electrons and aiding the saturation process. Note that the intensity peaks of the series of small radiation pulses emitted by the electron pulse are smaller than the steady-state saturation intensity $|A|_{sat}^2 \simeq 1.4$.

In order to test for Superradiance as defined in Ref.⁽²⁾ we plot the peak intensity I_P — in units of $|A|^2$ — of the first pulse emitted by the electron pulse, for various values of ρ^2 . This requires a separate run of the computer simulation for each value of ρ^2 , (ρ is the only parameter that was changed in the separate runs). Any superradiant emission will then exhibit a linear dependence of I_P on ρ^2 ($|E|_o^2$ is then proportional to the square of the electron density n_e).

In Fig 4. we performed six computer runs for six values of ρ^2 , with $N_o = 180$ and $N_b = 3$. These values of ρ^2 correspond to values of K in the range 1.7–6. A clear linear type dependence is seen, indicating superradiant emission of radiation. We note, however, that the linearity is not perfect with increasing ρ^2 (K^{-1}). This is because — as ρ^2 increases — the S.R. behaviour diminishes and tends to the steady-state behaviour, where $I_P \propto \rho^0$, *i.e.* no ρ^2 dependence.

This is seen more clearly in Fig.5 — where $N_o = 180$ and $N_b = 6$ — for larger values of ρ^2 — corresponding to values of K between 0.25 and 6 — with I_P tending to “flatten out” to the $|A|_{sat}^2$ value of 1.4, completing the transition from S.R. to steady-state (S.S.) regime.

We note then that the system may exhibit steady-state — or “long pulse” — behaviour even with a large slippage parameter, (here $S = 30$), as with sufficient gain radiation may saturate passing through the electron pulse. We conclude that the slippage parameter alone does not define the long or short pulse regions, the gain G must also be specified, this being incorporated in an expression for $K = S/G$.

Perhaps the most noticeable difference between the S.R. and S.S. regimes is observed when comparing the plots of E_L as a function of the position in the wiggler (that is, the dimensionless time τ).

Whereas in the long pulse (S.S.) limit the value of E_L never becomes greater than the $|A|_{sat}^2 \simeq 1.4$, in the S.R. regime it is seen (see Fig. 6.) that energy is extracted from the electrons at an almost constant rate. This is in full agreement with the theory exposed in Ref.⁽²⁾.

In the transition region between S.R. and S.S., energy extraction can be greater than the S.S. saturation value of 1.4; however, it does not occur at a constant rate and tends to a maximum value (see Fig. 7).

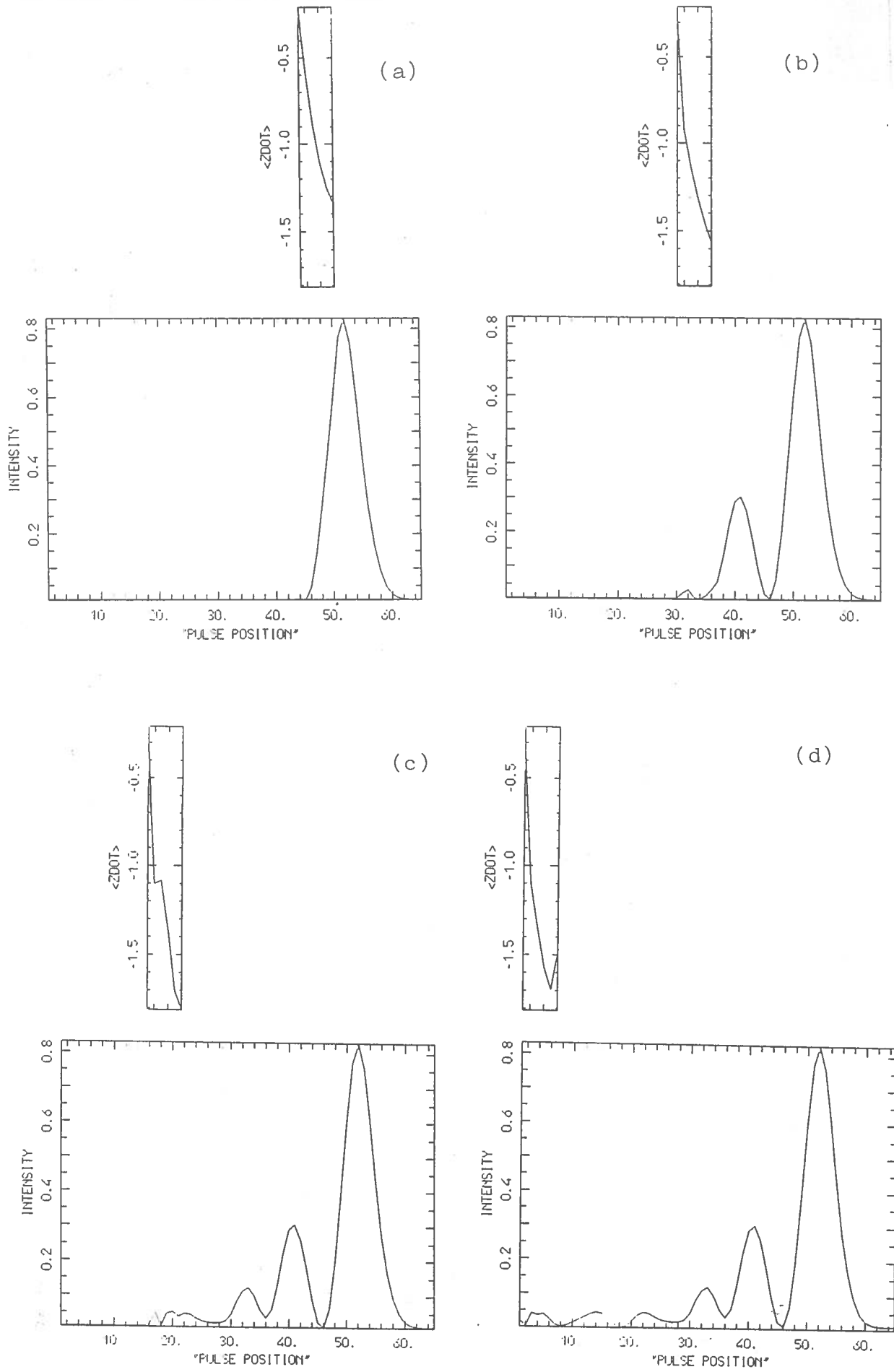


Fig.3. Radiation and electron pulses after N_P wiggler periods are shown in a) to d) for $N_P = 15, 30, 45, 60$ respectively. $N_o = 60$, $N_b = 6$ and $G = 20$, $|A(t = 0)|^2 = 10^{-2}$. A "Top hat" electron density function was used — $f(\bar{z}_1) = 1$ over the electron pulse.

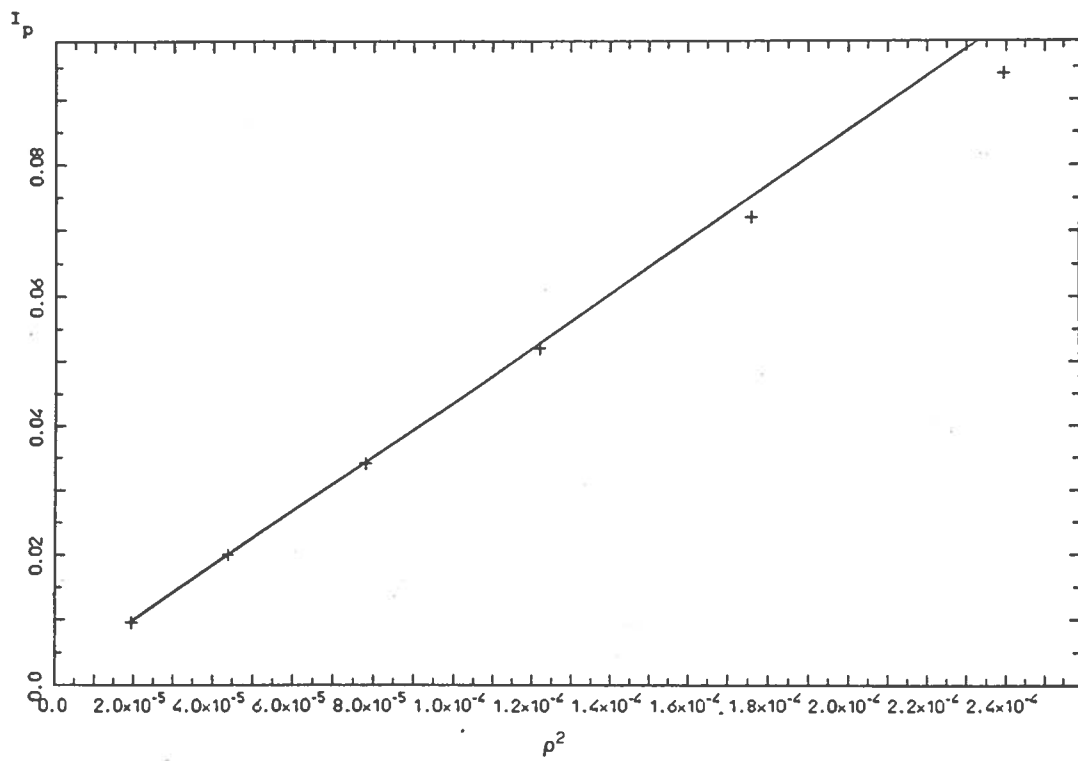


Fig. 4 I_P as a function of ρ^2 for $N_o = 180$, $N_b = 3$ and $|A(t = 0)|^2 = 10^{-3}$ over the radiation pulse.

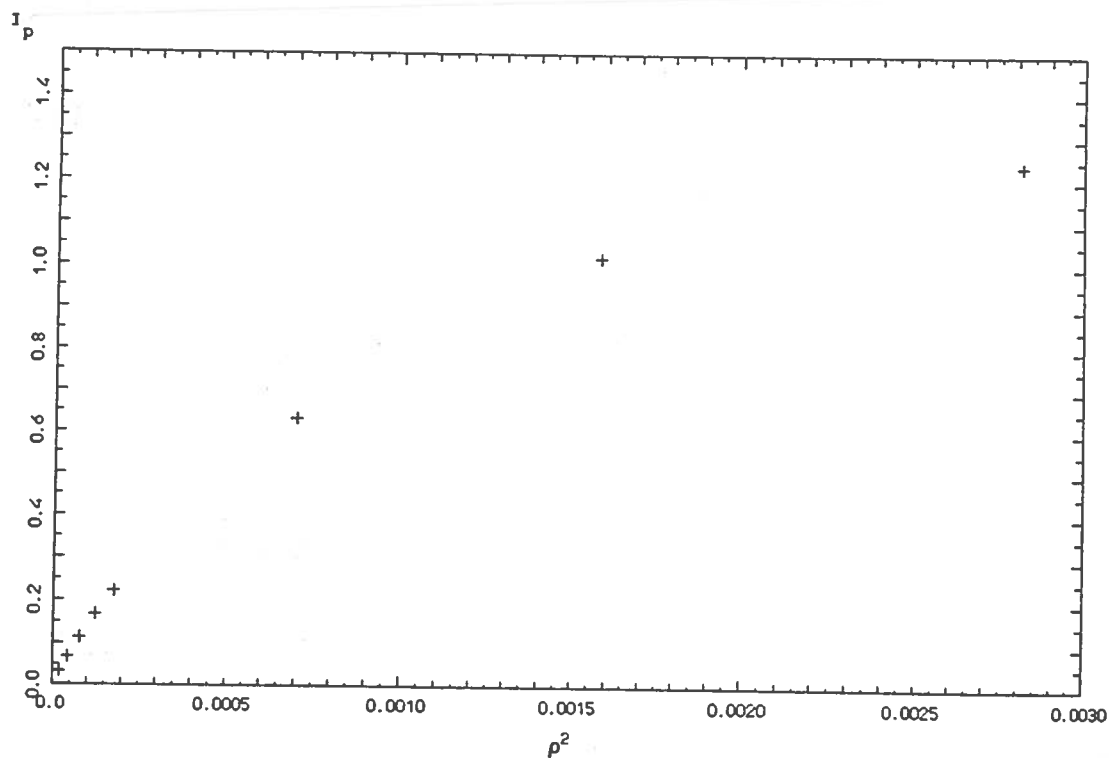


Fig. 5 I_P as a function of ρ^2 for $N_o = 180$, $N_b = 6$ and $|A(t = 0)|^2 = 10^{-3}$ over the radiation pulse.

5. - DISCUSSION

We use the "superradiant parameter", $K = L_b/L_c$, to define the long and short pulse regimes in the high-gain single-pass FEL. When $K \ll 1$ the system operates in the long pulse regime, and for $K > 1$ in the short pulse one.

We observe that previous theories for long pulses, (steady-state theories), do not describe fully the

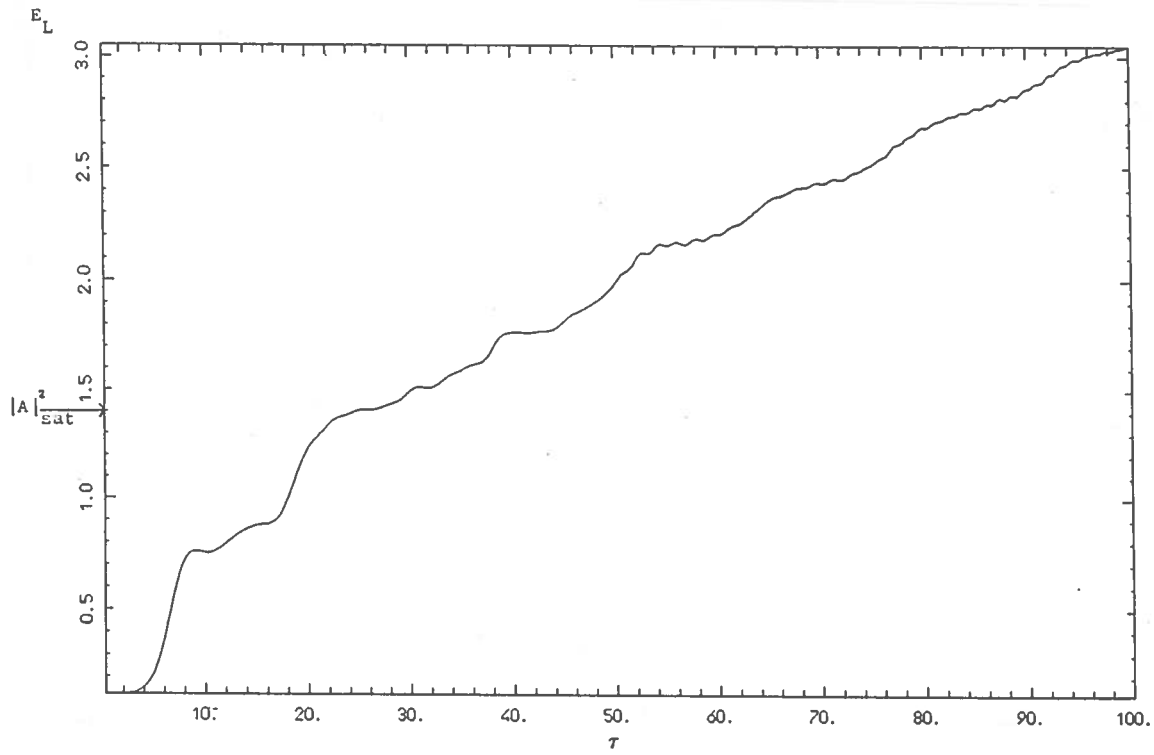


Fig.6. E_L as a function of dimensionless time through the wiggler in the superradiant regime. $N_o = 360$, $N_b = 3$, $G = 100$, $f(\bar{z}_1) = 1$ over the electron pulse and $|A(t=0)|^2 = 10^{-3}$ over the radiation pulse.

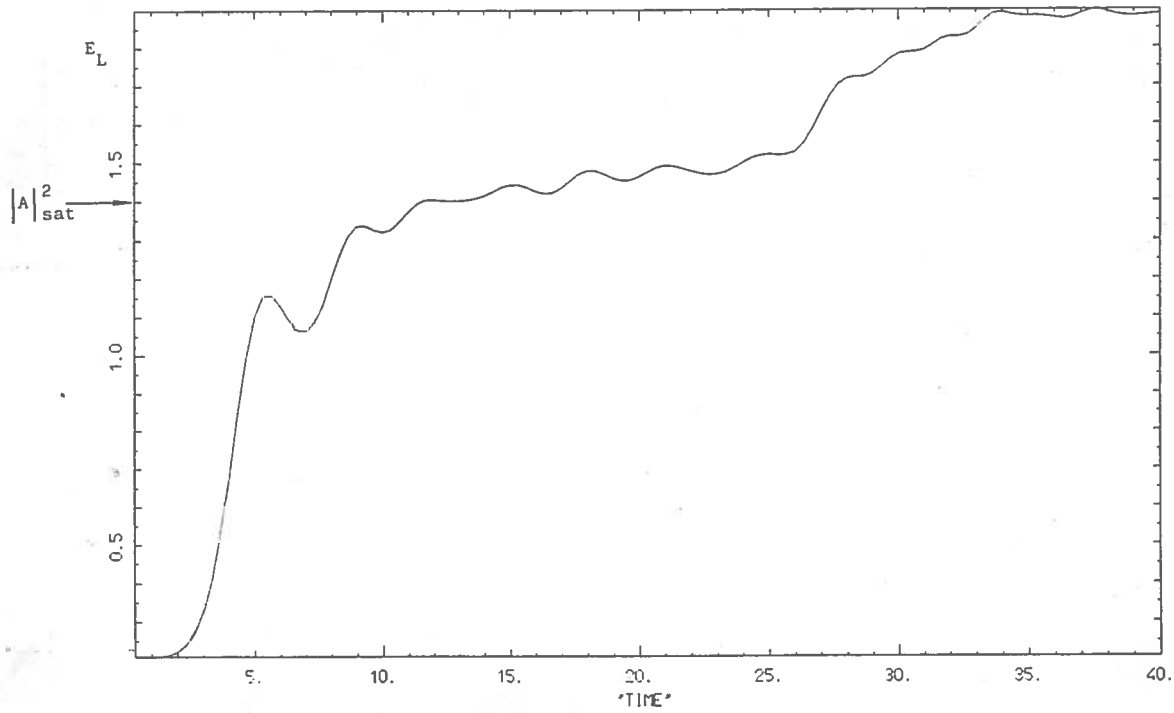


Fig.7. As in Fig. 6 but for the parameters of the pulse series shown in Fig. 3, with a longer undulator giving $G = 40$ ($N_o = 120$).

radiation output from the FEL: there is always a trailing region of the pulse in which the slippage effects give rise to the previously unreported spiking behaviour. We speculatively call this spiking a "Superradiant Synchrotron Instability". Clearly; however, further analysis of these spiked pulses is required, though we note here that preliminary work has shown a quasi-linear dependence on ρ^2 suggesting a superradiant type process.

Although the spikes can produce large differences from previous work in attainable peak intensities, the energy extracted from the electrons remain virtually unchanged from the steady-state state theories.

In the short pulse regime — with $K > 1$ — by computational modeling of the electron-radiation pulses we have showed for the first time the superradiant effect in the High-Gain Single-Pass FEL.

Energy extraction from the electrons is increased considerably in this regime and for the superradiant regime — $K > 1$ — energy is continuously extracted from the electrons.

6. - ACKNOWLEDGEMENTS

The authors would like to thank A.M.Sessler, C.Pellegrini and S.Krinski for helpful conversations and suggestions relating to the work presented here.

7. - REFERENCES

- (1a) R.Bonifacio, C.Pellegrini and L.Narducci, *Optics Comm.* **50** (1984) 373.
- (1b) T.J.Orzechowsky *et al.* *Phys. Rev.Lett.* **54** (1985) 889.
- (2) R.Bonifacio and F.Casagrande, *Nucl. Instr. and Meth.* **A239** (1985) 19.
- (3) R.Bonifacio, F.Casagrande and C.Pellegrini, *Optics Comm.* **61** (1987) 55.
- (4) W.B.Colson, *Nucl. Instr. and Meth.* **A250** (1986) 168.
- (5) S.SYu *et al.* preprint Lawrence Livermore National Laboratory, to appear in *Proceedings Eight International Free Electron Laser Conference.*